Efficient silicon nitride grating coupler with distributed Bragg reflectors

Huijuan Zhang,[1*] Chao Li,[1] Xiaoguang Tu,[1] Junfeng Song,[1,2] Haifeng Zhou,[1] Xianshu Luo,[1] Ying Huang,[1] Mingbin Yu,[1] and G. Q. Lo[1]

[1]*Institute of Microelectronics, A*STAR (Agency for Science, Technology and Research), 11 Science Park Road, Singapore Science Park II, 117685, Singapore*

[2]*State Key Laboratory on Integrated opto-electronics, College of Electronic Science and Engineering, Jilin University, Changchun, 13002, China*

[*]*zhangh@ime.a-star.edu.sg*

Abstract: In this paper we have designed, fabricated and characterized a high efficiency Silicon nitride grating coupler at 1490 nm. Distributed Bragg reflectors as bottom mirrors are employed to improve the coupling efficiency by reflecting the downward traveling light. The peak coupling efficiency obtained is about −2.5 dB and the 1-dB bandwidth is 53 nm. The fabrication process is CMOS-compatible and is ready to be integrated with photonic circuits.

OCIS codes: (130.3120) Integrated optics devices; (230.7380) Waveguides, channeled; (050.2770) Gratings.

References and links

1. W. Bogaerts, P. Dumon, D. V. Thourhout, D. Taillaert, P. Jaenen, J. Wouters, S. Beckx, V. Wiaux, and R. G. Baets, "Compact wavelength-selective functions in silicon-on-insulator photonic wires," IEEE J. Sel. Top. Quantum Electron. **12**(6), 1394–1401 (2006).
2. Y. A. Vlasov and S. J. McNab, "Losses in single-mode silicon-on-insulator strip waveguides and bends," Opt. Express **12**(8), 1622–1631 (2004).
3. S. K. Selvaraja, P. Jaenen, W. Bogaerts, D. V. Thourhout, P. Dumon, and R. Baets, "Fabrication of photonic wire and crystal circuits in silicon-on-insulator using 193-nm optical lithography," J. Lightwave Technol. **27**(18), 4076–4083 (2009).
4. T.-Y. Liow, K.-W. Ang, Q. Fang, J.-F. Song, Y.-Z. Xiong, M.-B. Yu, G.-Q. Lo, and D.-L. Kwong, "Silicon modulators and germanium photodetectors on SOI: monolithic integration, compatibility and performance Optimization," IEEE J. Sel. Top. Quantum Electron. **16**(1), 307–315 (2010).
5. T. Shoji, T. Tsuchizawa, T. Watanabe, K. Yamada, and H. Morita, "Low loss mode size converter from 0.3µm square Si wire waveguides to single mode fibres," Electron. Lett. **38**(25), 1669–1670 (2002).
6. Q. Fang, J. Song, X. Luo, M. Yu, G. Lo, and Y. Liu, "Mode-size converter with high coupling efficiency and broad bandwidth," Opt. Express **19**(22), 21588–21594 (2011).
7. V. R. Almeida, R. R. Panepucci, and M. Lipson, "Nanotaper for compact mode conversion," Opt. Lett. **28**(15), 1302–1304 (2003).
8. D. Taillaert, W. Bogaerts, P. Bienstman, T. F. Krauss, P. Van Daele, I. Moerman, S. Verstuyft, K. De Mesel, and R. Baets, "An out-of-plane grating coupler for efficient butt-coupling between compact planar waveguides and single-mode fibers," IEEE J. Quantum Electron. **38**(7), 949–955 (2002).
9. D. Taillaert, F. Van Laere, M. Ayre, W. Bogaerts, D. Van Thourhout, P. Bienstman, and R. Baets, "Grating couplers for coupling between optical fibers and nanophotonic waveguides," Jpn. J. Appl. Phys. **45**(8A), 6071–6077 (2006).
10. B. Wang, J. H. Jiang, and G. P. Nordin, "Embedded, slanted grating for vertical coupling between fibers and silicon-on-insulator planar waveguides," IEEE Photon. Technol. Lett. **17**(9), 1884–1886 (2005).
11. F. Van Laere, G. Roelkens, M. Ayre, J. Schrauwen, D. Taillaert, D. Van Thourhout, T. F. Krauss, and R. Baets, "Compact and highly efficient grating couplers between optical fiber and nanophotonic waveguides," J. Lightwave Technol. **25**(1), 151–156 (2007).
12. D. Vermeulen, S. Selvaraja, P. Verheyen, G. Lepage, W. Bogaerts, P. Absil, D. Van Thourhout, and G. Roelkens, "High-efficiency fiber-to-chip grating couplers realized using an advanced CMOS-compatible Silicon-On-Insulator platform," Opt. Express **18**(17), 18278–18283 (2010).
13. D. Taillaert, P. Bienstman, and R. Baets, "Compact efficient broadband grating coupler for silicon-on-insulator waveguides," Opt. Lett. **29**(23), 2749–2751 (2004).
14. X. Chen, C. Li, C. K. Y. Fung, S. M. G. Lo, and H. K. Tsang, "Apodized waveguide grating couplers for efficient coupling to optical fibers," IEEE Photon. Technol. Lett. **22**(15), 1156–1158 (2010).
15. M. Antelius, K. B. Gylfason, and H. Sohlström, "An apodized SOI waveguide-to-fiber surface grating coupler for single lithography silicon photonics," Opt. Express **19**(4), 3592–3598 (2011).

16. C. Li, H. Zhang, M. Yu, and G. Q. Lo, "CMOS-compatible high efficiency double-etched apodized waveguide grating coupler," Opt. Express **21**(7), 7868–7874 (2013).
17. G. Maire, L. Vivien, G. Sattler, A. Kaźmierczak, B. Sanchez, K. B. Gylfason, A. Griol, D. Marris-Morini, E. Cassan, D. Giannone, H. Sohlström, and D. Hill, "High efficiency silicon nitride surface grating couplers," Opt. Express **16**(1), 328–333 (2008).
18. S. C. Mao, S. H. Tao, Y. L. Xu, X. W. Sun, M. B. Yu, G. Q. Lo, and D. L. Kwong, "Low propagation loss SiN optical waveguide prepared by optimal low-hydrogen module," Opt. Express **16**(25), 20809–20816 (2008).
19. M. Melchiorri, N. Daldosso, F. Sbrana, L. Pavesi, G. Pucker, C. Kompocholis, P. Bellutti, and A. Lui, "Propagation losses of silicon nitride waveguides in the near-infrared range," Appl. Phys. Lett. **86**(12), 121111 (2005).
20. C. R. Doerr, L. L. Buhl, L. Chen, and N. Dupuis, "Monolithic flexible-grid 1×2 wavelength-selective switch in silicon photonics," J. Lightwave Technol. **30**(4), 473–478 (2012).
21. C. R. Doerr, L. Chen, Y.-K. Chen, and L. L. Buhl, "Wide bandwidth silicon nitride grating coupler," IEEE Photon. Technol. Lett. **22**(19), 1461–1463 (2010).
22. H. Zhang, C. Li, X. Tu, X. Luo, M. Yu, and P. G.-Q. Lo, "High efficiency silicon nitride grating coupler," Appl. Phys., A Mater. Sci. Process. **115**(1), 79–82 (2014).
23. H. Zhang, C. Li, X. Tu, X. Luo, M. Yu, and P. G.-Q. Lo, "High efficiency silicon nitride grating coupler with DBR," in Optical Fiber Communication Conference and the National Fiber Optic Engineers Conference (OFC/NFOEC) (2014), p. Th1A.4.
24. W. S. Zaoui, A. Kunze, W. Vogel, M. Berroth, J. Butschke, F. Letzkus, and J. Burghartz, "Bridging the gap between optical fibers and silicon photonic integrated circuits," Opt. Express **22**(2), 1277–1286 (2014).

1. Introduction

Silicon-on-insulator (SOI) has been considered as a promising platform for ultra-compact photonic circuits, thanks for its strong light confinement and CMOS compatibility [1–4]. There has been intensive work to develop reliable and efficient optical couplers for efficient light coupling into submicron size waveguides [5–7]. Grating coupler is an attractive candidate to replace edge coupler for allowing wafer-level testing [8–10]. Inspiring developments for Silicon (Si) grating coupler have been reported by various groups [11,12]. The typical performance on a 220 nm SOI platform is about 5 dB coupling loss. By employing an overlay layer or apodized grating, the coupling efficiency has been improved to less than 2 dB [13–16].

Silicon nitride (Si_3N_4) has a refractive index of ~2.0, which is significant smaller than Si, yet it still allows for highly compact device footprint [18,19]. It has been a promising alternative material for integrated photonic circuits, given the better tolerance to phase error, lower insertion loss, and better thermal stability comparing with Si [20]. However, there are few reports for Si_3N_4 grating coupler. The reported coupling efficiency for Si_3N_4 grating coupler are only −4.2 dB at 1550nm [21] and −5.2 dB at 1490nm [22].

Here we report the design, fabrication and characterization of Si_3N_4 grating coupler with bottom dielectric mirror. By employing distributed Bragg reflectors (DBR), the coupling efficiency for Si_3N_4 grating coupler is greatly improved. The device is fabricated using CMOS compatible processes. The preliminary result was first reported in Optical Fiber Communication Conference and the National Fiber Optic Engineers Conference 2014 and this paper presents more comprehensive results and discussions [23].

2. Simulation and design

In our previous work in [22], it is noted that the designed fully etched Si_3N_4 grating couples light equally to both top and bottom directions, which results in a 3-dB excess loss. To eliminate this undesirable loss, a bottom mirror is desired to reflect the down-travelling light upwards. Metallic mirror has been used as bottom mirror for its high reflectivity [24]. However, it is not preferred due to its fragility at high temperature and may not be compatible with other photonic devices. Dielectric DBR is chosen for the process readiness in CMOS line, the stableness at high temperature and the ability to be integrated with other active devices.

Figure 1(a) shows the cross section view of a fully etched Si_3N_4 grating coupler with two periods of DBRs on a Si substrate with a buried oxide (BOX) layer. The grating coupler is also covered by SiO_2 as upper cladding. To satisfy the Bragg condition at first order diffraction, $\frac{1}{\Lambda}=\frac{n_{eff}}{\lambda}-\frac{n_c \sin\theta}{\lambda}$, where n_{eff} is the effective index of the grating, n_c is the refractive index of cladding material, θ is the coupling angle respect to the normal to the grating surface and λ is the center wavelength, we employ two-dimensional (2D) finite-difference time-domain (FDTD) numerical simulations to investigate coupling efficiency for such grating structures [16]. In simulation, the refractive indices of Si_3N_4, amorphous Si and oxide are 2.0, 3.45 and 1.45, respectively. The grid size is 20 nm and the input light wavelength is set at 1490 nm. Each period of DBR consists of a high index material, amorphous Si and a low index material, SiO_2. The thickness of amorphous Si and SiO_2 are calculated according to $t=\frac{\lambda}{4n}$, where t and n is thickness and refractive index of the layer and λ is the incident wavelength. The film thickness is therefore set as 108 nm and 257 nm, respectively. The reflectivity of such DBR is as good as > 94.8% for wavelength ranging from 1400 nm to 1600nm. The reflectivity spectrum and light profile of the grating coupler with DBR are shown in Fig. 1(b). Figures 1(c) and 1(d) show the reflectivity spectrum change respect with variations of Si film thickness and SiO_2 film thickness, respectively. The scanning step for thickness variation is 10 nm. It is seen that variation of Si film thickness has larger impact than that of SiO_2, which is attributed to its higher index. The overall tolerance for thickness variation is considered to be very good as the reflectivity remains > 90% even with a 30 nm variation of Si film thickness. Hence, the material combination chosen for our DBR is very robust with high fabrication tolerance.

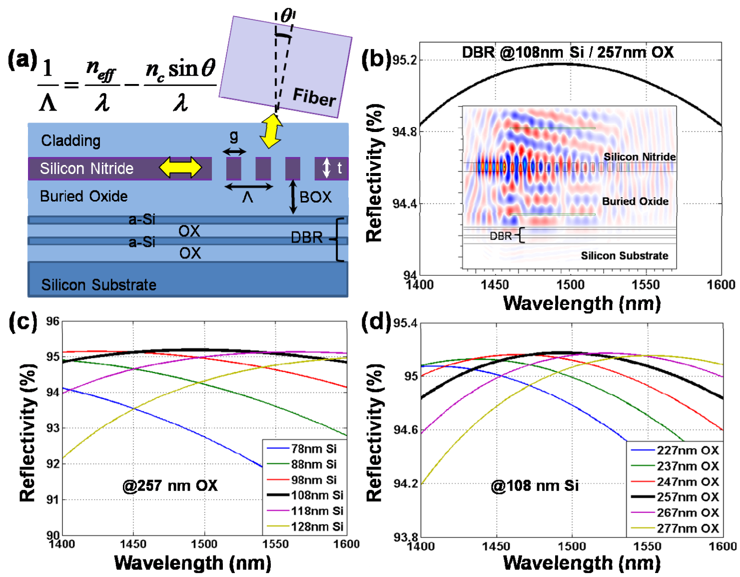

Fig. 1. (a) Schematic of a Si_3N_4 grating coupler with DBR; (b) reflectivity spectrum of designed DBR. Inset is the light propagating profile of the grating coupler with DBR; (c) reflectivity spectrums v.s. Si film thickness variation when SiO_2 film is 257 nm; (d) reflectivity spectrums v.s. SiO_2 film thickness variation when Si film is 108 nm.

Parameters including grating period Λ, filling factor and BOX thickness are evaluated to optimize coupling strength with a desired coupling angle θ. The filling factor is defined as the ratio of the remaining grating width g to the grating period Λ. Coupling efficiency between the fiber and waveguide is calculated using the power coming out from the grating coupler versus the total power from the light source. The oxide upper cladding thickness is 2 µm. 2D FDTD simulation results are shown in Figs. 2(a)-(c) to obtain a Si_3N_4 grating coupler with optimized parameters: (a) coupling efficiency as a function of period; (b) coupling efficiency as a function of filling factor; (c) coupling efficiency as a function of BOX thickness. Λ is chosen to obtain out-coupling light with a preferred coupling angle, θ = 8°. The optimum parameters are found as following: Λ = 1.05 μm, filling factor = 0.55 and BOX thickness = 2.6 μm. Given these optimum parameters, we obtain a low coupling loss of −2.32 dB, corresponding to a coupling efficiency of ~58.6% at wavelength of 1479 nm. This much improved coupling loss is 2.72 dB better than that of a grating coupler without DBR. (Fig. 2(d)) The 1-dB bandwidth is as wide as 102 nm and 93 nm for grating with and without DBR respectively, which is significantly larger than Si grating coupler due to the lower index of Si_3N_4 [21].

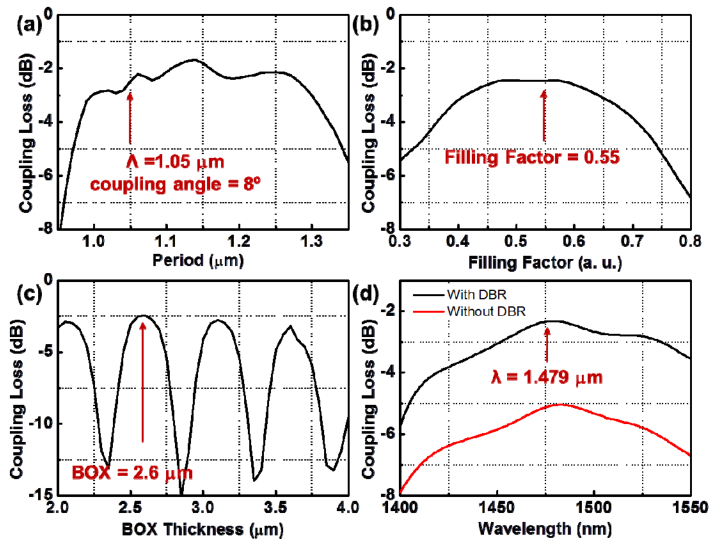

Fig. 2. Simulations for coupling loss with respect to (a) period, (b) filling factor, (c) BOX thickness and (d) wavelength. Coupling loss of designed grating coupler without DBR is also shown in (d) (red line).

3. Fabrication and characterization

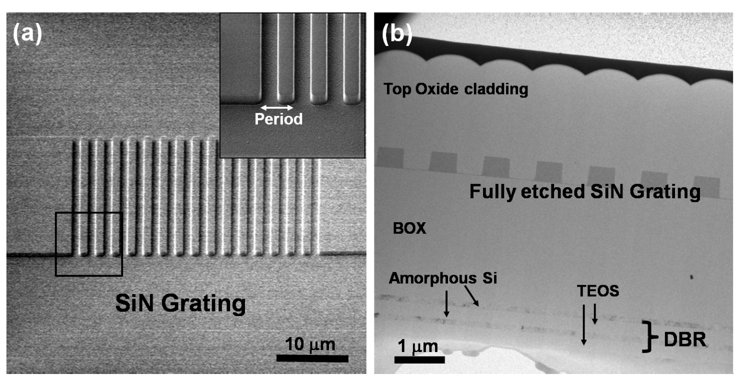

Fig. 3. (a) SEM image of a Si_3N_4 grating coupler. Inset at right corner is the zoom-in view of the indicated area. Scale bar in the inset is 1μm. (b) Cross section view of the device.

The grating couplers with bottom mirrors were fabricated on an 8-inch Si wafer. Two periods of DBR consisting of alternating layers of SiO_2 (257 nm) and amorphous Si (108 nm) were deposited by low pressure chemical vapor deposition (LPCVD) system. A BOX layer (2.7 μm) was then deposited using plasma enhanced vapor deposition system (PECVD) followed

#214625 - $15.00 USD Received 23 Jun 2014; revised 30 Jul 2014; accepted 4 Aug 2014; published 2 Sep 2014

by a chemical mechanical polishing step to achieve wafer flatness and the optimized thickness of 2.6 μm. A Si_3N_4 layer with 400 nm thickness for waveguide was deposited by LPCVD. The waveguide and grating structures were first patterned by optical deep UV lithography using a Nikon Scanner and then fully etched using reactive ion etching (RIE) to BOX surface. Next, 2 μm SiO_2 was deposited using PECVD on the wafer as the top cladding. Figure 3(a) shows the image of the Si_3N_4 grating coupler with 15 periods fabricated before cladding deposition. The cross section of the device is shown in Fig. 3(b).

The coupling efficiency of Si_3N_4 grating couplers fabricated is characterized with a fiber-to-fiber measurement. Two identical grating couplers at input and output ends are connected by a straight waveguide. A pair of adiabatic linear tapers with a length of 500 μm is used to gradually taper the 12-μm-wide grating region to a 1-μm-wide waveguide section. The total length of each device is 2.8 mm. Fiber-to-fiber transmission is measured to characterize the insertion loss. A tunable laser (Agilent 8164B) was employed as the input light source and a polarization controller is connected to the laser source to tune the input light to be TE-polarization. Light is launched into the input coupler using a cleaved single mode fiber. The scanning range is from 1400 to 1550 nm with a resolution of 0.01 nm. The output light is captured by another single mode fiber connected to a spectrum analyzer. Both fibers are tilted at 8° (unless stated otherwise) and no index matching fluid is applied.

All the measured data are normalized to the insertion loss from the laser source and the polarizer, which is about 0.9 dB and 0.6 dB respectively. The possible additional loss from the cleaved fibers and connectors are taken into account for the final coupling loss as it is very hard to decouple this loss. The measured propagation loss for the straight single-mode strip Si_3N_4 waveguide with a width of 1 μm was ~0.72 dB/cm. The ~2.7 mm waveguide and gradual tapers are thus treated as lossless given the negligible propagation loss. In addition, it is assumed that the input and output grating coupler have the same coupling loss for the symmetric testing setup.

Figure 4(a) shows the measured coupling loss for Si_3N_4 grating coupler as a function of period versus the filling factor. It is observed that a filling factor of 55% (refers to the unetched part as defined) is optimal and the spectrum obtained agrees well with the simulation result. Variation of period (in a step of 50 nm) leads to large increment of coupling loss as the Bragg condition is no longer satisfied. In addition, Fig. 4(b) shows the measured coupling loss as a function of wavelength respect with filling factors of 50%, 55%, 60% and 65%. It is observed that the tolerance for various filling factor, which can be translated to dimension variation in fabrication, is very good. An increment of 5% filling factor from 55% to 60%, corresponding to ~52.5 nm change in grating width, results a merely additional 0.5 dB coupling loss.

Figure 4(c) shows the measured coupling loss as a function of wavelength respect with tiled angles of 7°, 8°, and 9°. The simulation result is also plotted in Fig. 4(c). The minimum coupling loss is −2.5 dB at 1484.3 nm. The coupling loss and center wavelength agrees very well with the simulation result of −2.32 dB at 1479 nm. The 1dB-bandwidth of the experimental data is 53 nm, which is smaller than the simulation value of 102 nm. It is seen that the coupling efficiency drops quite fast at a longer wavelength (>1525 nm) comparing with the simulation spectrum. It should be noted that in simulation, the numerical power loss is considered only to calculate coupling efficiency, while the mode overlapping between waveguide and optical fiber is not taken into account. This discrepancy in coupling loss and bandwidth should be attributed to the mode mismatching, possible imperfect etched profile and DBR film thickness variation in fabrication. The coupling loss of a grating coupler having same dimension design without DBR is also measured at various tiled angles and shown in Fig. 4(d). The minimum coupling loss is −4.7 dB at 1481 nm with a 1dB-bandwidth of 59 nm. The measured fluctuations of grating with DBR are larger than that of grating without DBR, which should be due to reflection from multiple surfaces of DBR films as well as multiple mode excitation at the taper.

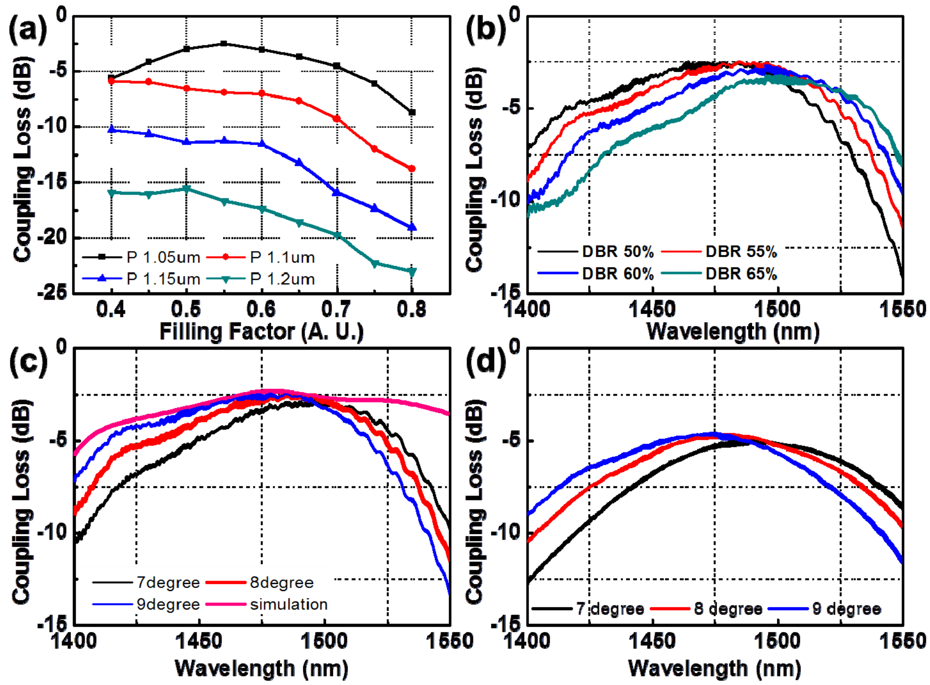

Fig. 4. (a) Coupling loss versus filling factor as a function of period. (b) Coupling loss versus wavelength as a function of filling function at 8°. (c) Coupling loss versus wavelength as a function of tiled angles and simulation result (pink). (d) Coupling loss versus wavelength as a function of tiled angles for a grating coupler without DBR.

4. Conclusion

In conclusion, we have experimentally demonstrated a high efficiency Si_3N_4 grating coupler with two periods of DBR as bottom mirror. Si_3N_4 grating coupler performance benchmark is shown in Table 1. Reference [17] reported a higher efficiency; however, the grating coupler is 40 µm wide and coupled to a free space beam with a relatively large diameter of ~30µm. The fabrication process is compatible with conventional CMOS technology using deep UV photolithography (248 nm). The measured minimum coupling loss is −2.5 dB, which corresponds to a 56.0% coupling efficiency. To the best of the researchers' knowledge, this is the best coupling efficiency demonstrated experimentally in Si_3N_4 grating for single mode fiber coupling.

Table 1. Silicon Nitride grating coupler performance benchmark

Ref.	Cent er λ (nm)	Si_3N_4 Thickness (nm)	Coupling loss (dB)	Remarks
[17]	1310	300	−2.2 (60%)	Large beam size (~30mm)
[21]	1550	400	−4.2	Alcatel-Lucent fabricated in IME
[22]	1490	400	−5.2	IME's platform
This work	**1490**	**400**	**-2.5**	**IME's platform**

Acknowledgment

This work was supported by the Science and Engineering Research Council of A*STAR (Agency for Science, Technology and Research), Singapore. The SERC grant number is 1323300001.

#214625 - $15.00 USD Received 23 Jun 2014; revised 30 Jul 2014; accepted 4 Aug 2014; published 2 Sep 2014